Journal of Structural Geology, Vol. 10, No. 2, pp. 183 to 192, 1988
Printed in Great Britain

0191-8141/88 $03.00 + 0.00

Displacement variation along thrust faults: implications for the development of large faults

MICHAEL A. ELLIS* and W. JAMES DUNLAP†

Department of Geology, University of Minnesota-Duluth, Duluth, MN 55812, U.S.A.

(*Received* 18 *May* 1987; *accepted in revised form* 19 *November* 1987)

Abstract—Displacement analyses along thrust faults of different maturity (or size) reveal maxima and minima, often associated with minor folding of the adjacent beds, between the tip points. The results show that these faults are segmented, and that they formed through the linkage of smaller (previously independent) faults, and (or) by propagation of a single fault affected by the existence of barriers. Points of potential linkage (marked by displacement minima) are fault bends or distinct fault breaks. Fault nucleation (marked by displacement maxima) occurs within the planar segments of a fault; only in one of eight examples is the nucleation point seen to occur at a fault bend.

Displacement variations along inferred or extrapolated regional-scale thrust faults show a variety of patterns, most of which involve constant displacement or a monotonic increase or decrease away from the basal décollement. These data are not considered to be as reliable as those from observed thrusts due to the necessary subjectivity involved in the extrapolation process.

In general, displacement variation appears to be a reflection of the symmetry of the thrust fault system, such that, for example, a flat-ramp geometry ending in a steep tip will show an asymmetrical displacement function skewed toward the surface, with a nucleation point *above* the basal décollement.

INTRODUCTION

THIS paper presents three sets of displacement patterns along thrust fault systems of different maturity (or size) which support the hypothesis of fault development whereby large faults develop through the linkage of smaller ones (Gretener 1972, Dunlap & Ellis 1986), and propagation and displacement is affected by the existence of barriers (King & Yielding 1984). Displacement variations between tip points show internal minima and maxima which may reflect barriers or points of fault linkage. We propose that both interpretations are possible, and that King and Yielding's (1984) scenario of thrust fault development be extended to include the coalescence of separate fault segments, a process which by its nature is confined to the early history of a large fault.

In addition, displacement patterns suggest that large thrust faults *do not* develop by stepping off a basal décollement, thence to cut neatly up section, leaving the footwall an inert and silent partner in the development of a thrust (e.g. Williams & Chapman 1983, Suppe 1985). In contrast, thrust faults nucleate *above* their sole thrust, and propagate up toward the surface, and down toward the flat. In other words, deformation in the footwall is an integral part of the formation of a thrust fault, and in the development of a fold and thrust belt, a point emphasized by Casey (1982, Tectonic Studies Group, Ann. Mtg.), and neglected in developmental models of fold and thrust belts.

ANALYSIS AND INTERPRETATION OF FAULT DISPLACEMENTS

Displacements along a fault are often referred to the distance between a cut-off point and a reference point (usually near the tip of the fault) in either the hangingwall or footwall (Williams & Chapman 1983). The nucleation point on the fault corresponds to the original site of the maximum-displaced horizon, but since displacements only record the relative motion across the fault, the exact position of the nucleation is unobtainable unless the absolute motion of some point is known. Nevertheless, the nucleation site can be found within the limits set by the maximum displacement. For example, if the footwall was immobile during development of a thrust fault, the nucleation point would be found by referring displacements to distances in the footwall (Fig. 1). Displacements referred to distances in the hangingwall would predict a nucleation point above its actual site; the error would be equal to the maximum displacement (Fig. 1). The opposite would be true if the

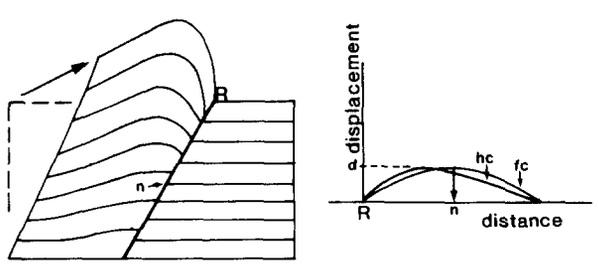

Fig. 1. Displacement distribution along a thrust fault where the footwall is fixed. The displacement–distance diagram (right) refers displacement to distances in the footwall (labeled fc) and hangingwall (labeled hc). The footwall curve accurately locates the nucleation point, *n* (maximum displacement, *d*), where the hangingwall curve misses by a distance equal to the maximum displacement.

*Present address: Center for Neotectonic Studies, Mackay School of Mines, University of Nevada-Reno, Reno, NV 89557, U.S.A.

†Present address: Department of Geology and Geophysics, University of Minnesota, Minneapolis, MN 55455, U.S.A.

hangingwall remained immobile. The best approximation to the nucleation site will be determined by referring displacements to distances halfway between hangingwall and footwall cut-offs. This amounts to assuming that both footwall and hangingwall enjoy similar deformation during fault development. If this is the case, then the modified analysis described here is an Eulerian description of displacement; we therefore label the resultant displacement–distance curve, PEDA (Pseudo-Eulerian Displacement Analysis).

The PEDA curve retains the uses of the original (in calculating total displacements, and the position of buried or eroded tips) and has the advantage, in our opinion, of giving a clearer reflection of displacement distribution along a fault. Some basic characteristics of the PEDA curve are as follows: symmetrical rates of displacement *and* fault propagation (about the nucleation point) will be reflected by a similarly symmetrical curve; asymmetrical fault propagation will be revealed by an asymmetrical curve and an off-centered displacement maximum; and asymmetrical displacement but symmetrical propagation will be shown by an asymmetrical curve but centred displacement maximum. These simple characteristics are strictly applicable to displacement distributions following a single seismic event.

The interpretation of displacement functions for multiple event faults is open to some ambiguity due to the assumed seismic history. The interpretations offered here are based on the concept of the 'characteristic earthquake' which states that faults tend to generate essentially the same size earthquake having a relatively narrow range of magnitudes near the maximum (Schwartz *et al.* 1981). A characteristic earthquake is expressed geologically as one of a generally constant displacement function. This view resembles the 'self-similar' concept adopted by King (1986) which describes the development of a fault in terms of the cumulative addition of displacement functions that are self-similar; in other words, each event is geometrically similar to the previous and next event, and the nucleation point (maximum displacement) is spatially fixed.

The form of the displacement function may also be influenced by differences in lithology. Muraoka and Kamata (1983) showed examples of displacement functions along normal faults in which changes in displacement gradient are apparently related to differences in material competency. This view is somewhat implicit in the description of the simple characteristics of the PEDA curve (see above) in which the form of the displacement function is dependent on both fault and displacement propagation, which are presumably partially dependent on lithology (or competency).

In each of the samples described below we have attempted to measure the displacement parallel to the displacement vector, although in none of the examples are we certain of this direction. This uncertainty should only affect interpretations concerned with absolute gradients of displacements, and should not affect interpretations derived from irregularities in the displacement function. This follows from the 'characteristic earthquake' concept in which displacement falls off smoothly from the nucleation point in all directions.

SAMPLE DESCRIPTIONS AND DISPLACEMENT VARIATIONS

Microfaults in mylonite

A thinly laminated, 0.5–2 mm, quartz–feldspar mylonite (Fig. 2) from Francis Peak, Wasatch Range, Utah, contains a high-angle thrust (reverse fault) approximately 5 cm in length, and inclined at 45° to the laminae. The fault is associated with an open, 5 cm wavelength, conical fold within the hangingwall above the tip zone (Fig. 2). A well-defined hinge line separates the fold from the planar mylonitic layering; we interpret this line as also the separation between undeformed and deformed mylonite. The geometry of the fold and associated(?) fault resembles the bow and arrow pattern recognized in many regional fold and thrust belts, and suggests that the displacement vector parallels the cut face in Fig. 2.

The fault comprises a complex of microfaults of variable length (mm to cm) with an average inclination of 45° to the laminae, although they vary from parallel to almost perpendicular to the laminae. Figures 3 and 4 show details of two microfaults and the displacement variation along their length. In one example (Fig. 3) a single displacement minimum coincides with a slight bend in the fault, separating two planar segments, each associated with a displacement maximum, or nucleation point, of similar magnitude. No microfolding is visible along this fault; displacement is transferred across the minimum without noticeable effect. Note the overall symmetry of the displacement.

The second example (Fig. 4) shows two displacement minima coincident with small breaks in the fault trace; the larger microfault comprises three small microfaults.

Fig. 2. Thrust fault complex (approximately 5 cm in length) within quartz–feldspar mylonite. Hinge line of conical fold runs from the nearest corner along the black line.

Fig. 3. Photomosaic of a segmented microfault (approximately 5 mm long) in the deformed mylonite and the appropriate displacement function. The displacement minimum occurs at a slight (but real) fault bend marked by a large dot. See text for discussion.

Fig. 4. Photomosaic of a segmented fault (approximately 7 mm long) in the deformed mylonite. Note the general asymmetry of the displacement function indicating a faster fault propagation toward the lower flat. The displacement minima coincide with breaks in the continuity of the fault. Microfolding is visible at both displacement maxima (nucleation points) and minima, but not at points in between (see also Fig. 5).

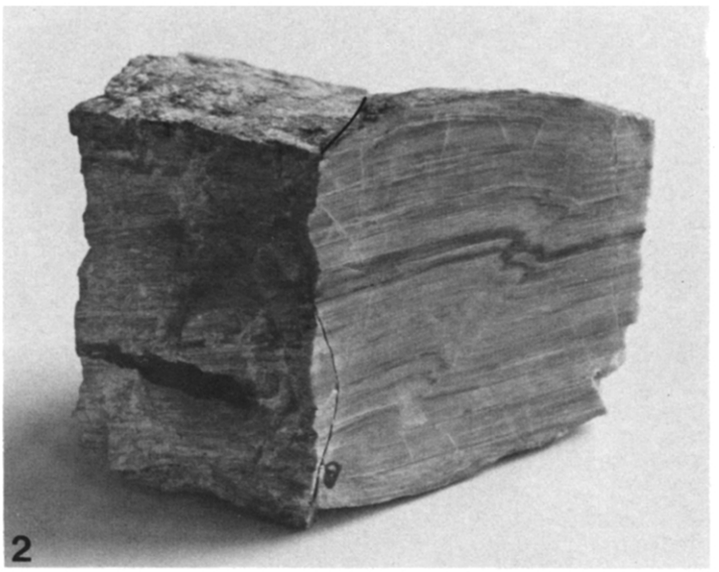
2

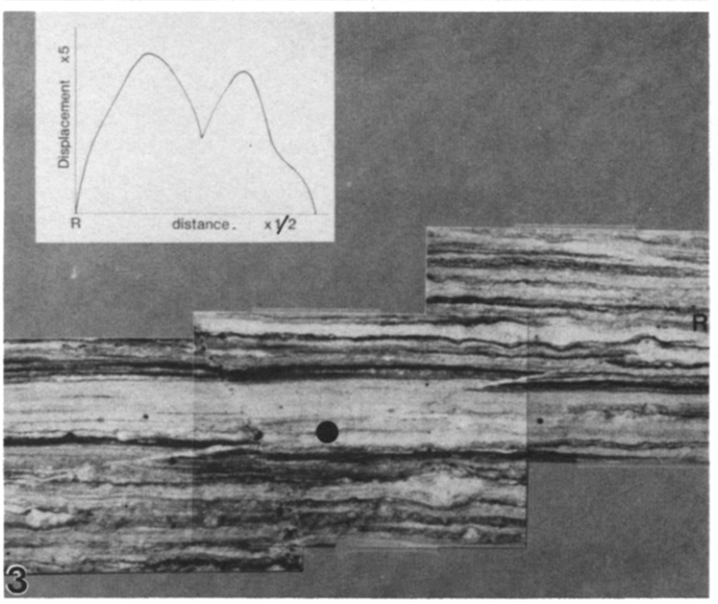
Displacement x5
R
distance.
x √2
R
3

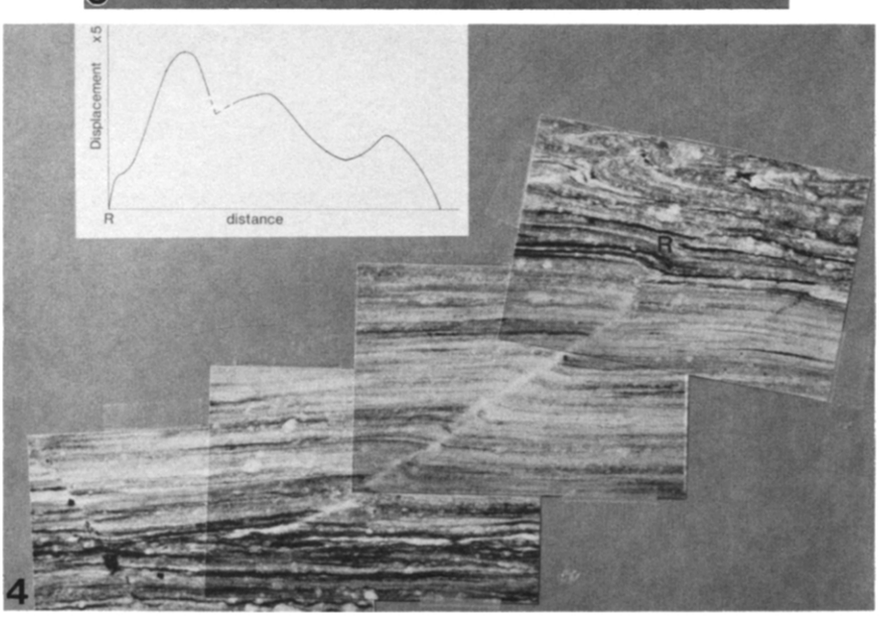
Displacement x5
R
distance
R
4

Figs. 2–4.

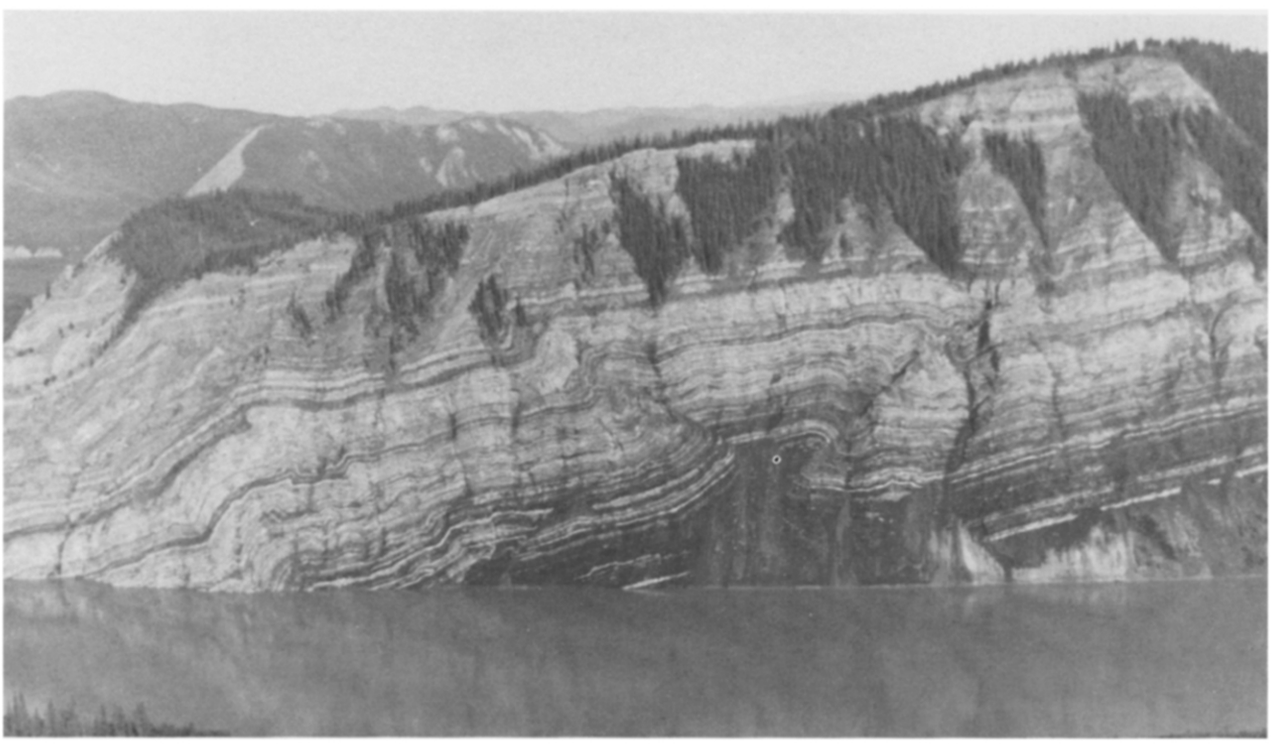

Fig. 6. Pop-up structure along the Yukon River, 19 km downstream from Eagle, Alaska. Cliff is vertical to the tree line, and is about 250 m (800 feet) high. The conjugate fault system is developed within Upper Devonian–Mississippian shales (dark colored) and carbonates (light colored). (Photograph courtesy of David G. Howell, USGS, Menlo Park, and reproduced with permission from American Association of Petroleum Geologists.)

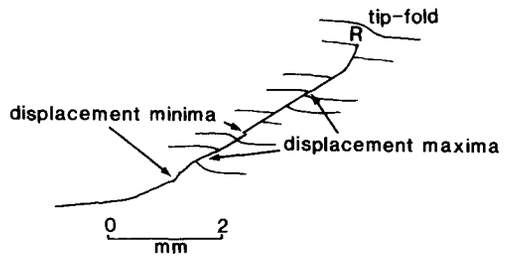

Fig. 5. Line drawing of the microfault in Fig. 4 showing some displaced horizons. Note the gentle flexure located either side of the maximum displacement and the apparent lack of off-fault deformation between the flexure and the tip points (see also Fig. 4). The flexure is interpreted as a response to the variable displacement along the fault.

Microfolds are (barely) visible at both displacement minima and (the two higher) maxima, but are noticeably absent at points in between (Fig. 5). Note the overall asymmetry in the displacement such that the displacement gradient is higher along the steeper part of the fault.

Pop-up in Alaska

The pop-up structure, located along the Yukon River, Alaska (Fig. 6), is developed within Upper Devonian–Upper Mississippian shales and carbonates, and comprises two conjugate faults and associated disharmonic folding. Displacement variation along the right fault (Fig. 7) reveals one distinct minimum (nearer the reference point) which coincides with a bend in the fault trace and with minor folding in adjacent beds. Two less distinct minima occur below this; the lower of which is associated with a minor fold. Displacement variation along the left fault (Fig. 7) reveals a single distinct minimum situated at one end of a fault bend. The two displacement maxima are of similar magnitude; that closer to the reference point separates a minor hangingwall–footwall anticline–syncline pair. The displacement curve shows an overall symmetry and an off-centred (average) maximum skewed toward the lower horizons.

Regional-scale thrust faults

Displacement analyses of large thrusts, mainly within the Cordilleran fold and thrust belt (Price & Fermor 1982, Mudge 1972, Royse *et al.* 1975), show a spectrum of results: displacements may consistently increase or decrease toward the surface with a variable degree of irregularity, remain constant, or show apparent internal maxima and minima. Four examples are shown in Figs. 8–10.

Displacement variation along the Fire Trail Thrust (Fig. 8), within the Wyoming–Idaho Thrust belt (Royse *et al.* 1975), shows a distinct maximum approximately 2500 m above the local décollement. The displacement maximum occurs within the Mississippian dolomite. Notice also that displacement falls off more rapidly on the upper side of the maximum, toward the blind tip, and the displacement maximum is off-centered. The additional strain required by the higher displacement gradient near the tip may explain the presence there of minor folding.

Displacement variation along an unnamed thrust within the hangingwall of the Fire Trail, near Auburn, Wyoming (Fig. 8), shows a steadily decreasing displacement away from the surface. It is possible that the point of nucleation is above the present horizon, or that the displacement rate was significantly asymmetrical. The 'Auburn' Thrust separates an anticline–syncline pair.

Displacement variation along the Turner Valley Thrust (Fig. 9), Alberta, Canada, shows a decrease in displacement toward the surface, and a maximum within the lower flat. Although no distinct internal minimum occurs, there is a jog in the displacement pattern close to the tip, which may reflect an apparent mistake in the original cross-section by Gallup (1951), later revised along this section of the fault (Gordy & Ferry 1975).

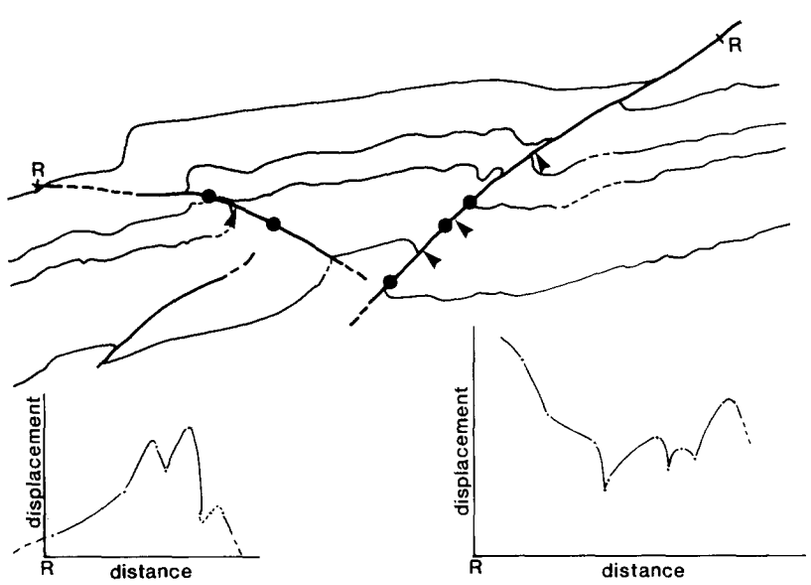

Fig. 7. Simplified line drawing, and displacement functions, of the conjugate fault system showing reference points, and displacement minima and maxima. Displacement is exaggerated on the vertical axis by a factor of 10. See text for discussion.

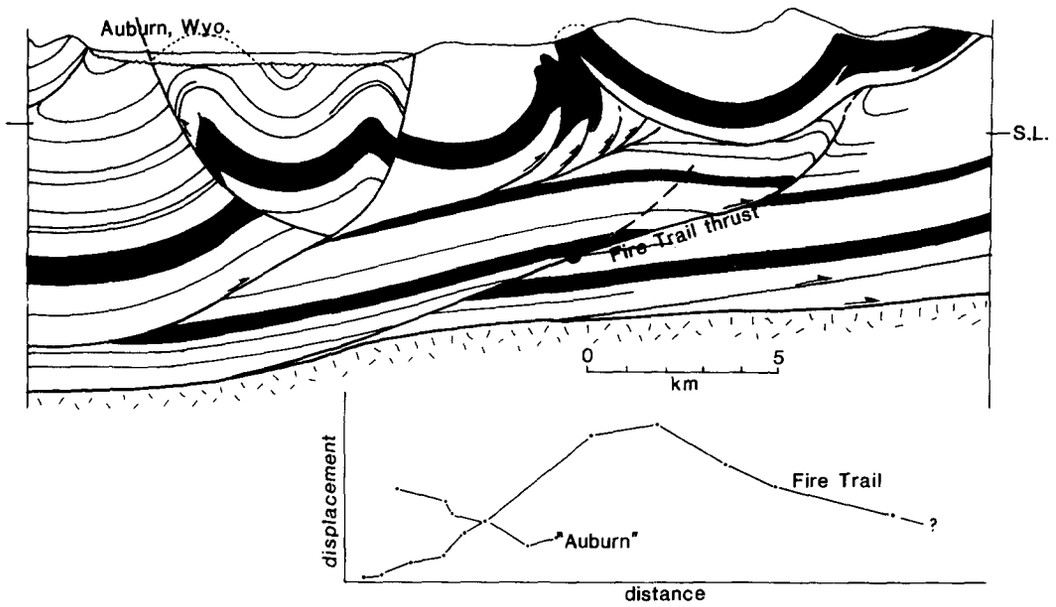

Fig. 8. Cross-section through part of the Wyoming–Idaho Thrust belt showing the Fire Trail and 'Auburn' Thrusts, among others (simplified after Royse *et al.* 1975). The dark stippled unit marks the Mississippian dolomite; the black the Nuggett sandstone. The displacement functions for the two named thrusts are shown at lower right. Note the general asymmetry of the Fire Trail displacement; location of the nucleation point is shown by large dot.

An unnamed but apparently well constrained cross-section of a thrusted anticline in Virginia (Badgley 1965, fig. 6.8, partly reproduced here as Fig. 10) shows an overall decrease in displacement toward the surface, with the hint of a maximum and similar displacement decrease toward the flat. The displacement maximum is associated with a tight fold, now separated, across the fault, but note also the gentle fold within the footwall. Maximum displacement is seen in the Middle Ordovician carbonate unit, which is enveloped by beds of shale.

INTERPRETATION

Fault segmentation and growth through linkage

The distribution of displacements along microfaults and their arrangements within the deformed mylonite show that these faults are segmented, propagate backwards and forwards, and may join to form larger faults. In one example (Fig. 3) the two fault segments display similar displacement functions. We interpret this as an

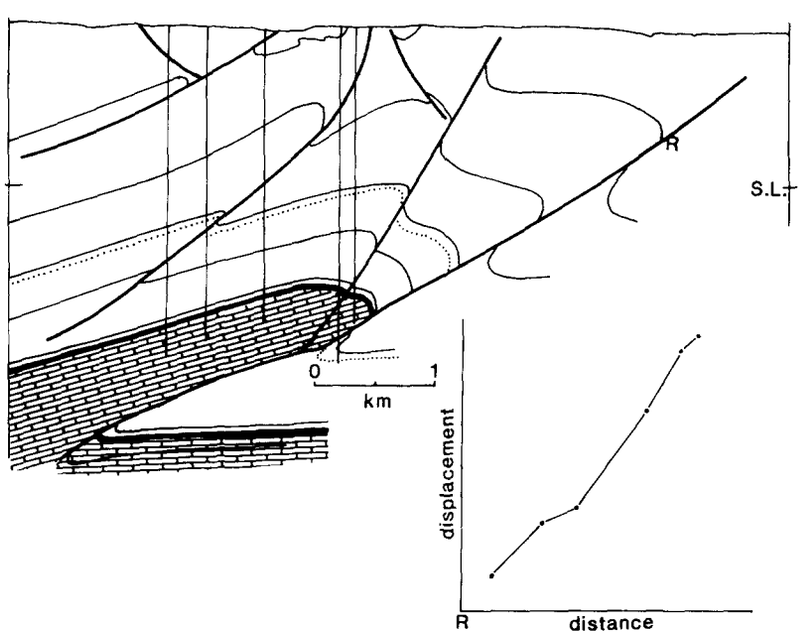

Fig. 9. Cross-section through the Turner Valley Thrust, Alberta, and its displacement function (simplified after Gallup 1951). The displacement function is insignificantly changed if the modified version of the cross-section by Gordy & Ferry (1975) is used.

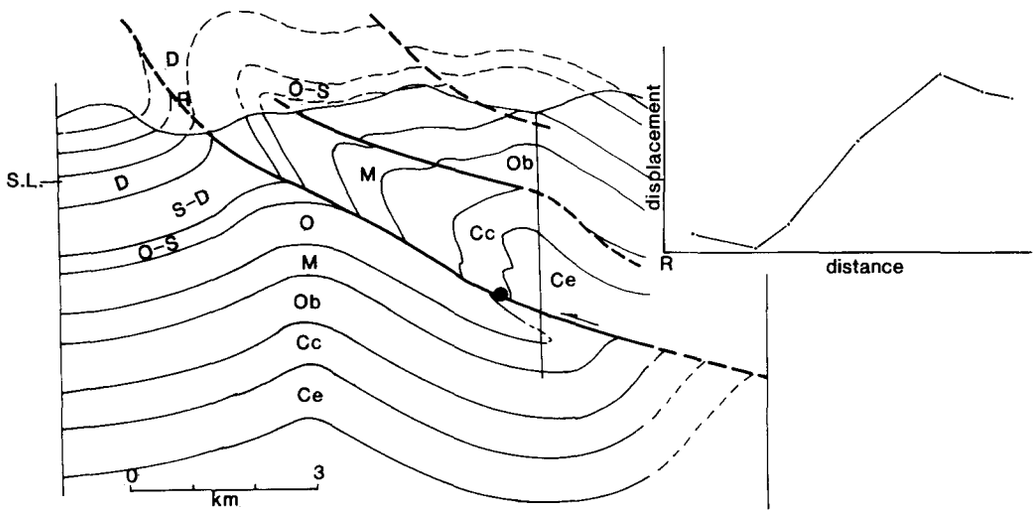

Fig. 10. Cross-section and displacement function for an unnamed thrust-fold pair in Virginia (simplified after Badgley 1965, fig. 6.8). Letters correspond to various Lower Palaeozoic horizons; M is a carbonate, and the two Ordovician units are shales. See text for discussion.

indication that two separate faults, of slightly different orientation, developed independently (but at about the same time) and subsequently joined. The symmetry of the displacement patterns suggests that propagation was symmetrical; this is probably due to the planar shape of the faults. The apparent absence of deformation around the link point (transferring and absorbing the displacement gradient) may be a function of the minimal total displacement, or that deformation is distributed around the whole fault as subtle folding or flexing (Watterson 1986).

The second example (Fig. 4) shows a displacement pattern that is more difficult to interpret. The internal displacement minima and maxima may reflect independently developed microfaults or segments separated by barriers. The overall displacement pattern bears a striking resemblance to that along the segmented thrust of the El Asnam earthquake of 1980 (King & Yielding 1984, compare their fig. 4 to our Fig. 4). In other words, it is possible that each segment of the microfault in Fig. 4 represents a new addition to the larger fault, and formed in response to a barrier. The barriers in this case are the fault bends (cf. King 1986). The overall asymmetry of the displacement may, on the other hand, simply reflect a faster fault propagation within the lower, flatter portion of the fault. This interpretation is supported by the geometry of the fault: the top section is oriented at a high angle to the mylonitic laminae, and presumably encountered greater resistance to fracture than the flatter, lower section of the fault (hence the fold at the higher tip where none exists at the lower tip).

Displacement distribution along the conjugate fault system (Fig. 6), or pop-up, reflects that in the deformed mylonite, the larger faults comprise segments of smaller faults. Whether the segmentation developed through independently developed faults or not is unknown. In one example (Fig. 7, left side) the two fault segments have similar maximum displacements which suggests (but does not necessitate) that each started independently but at the same time. The displacement minimum, or link point, is situated at the end of a long bend between fairly planar segments, but the higher nucleation point is also situated within the fault bend. This is not observed in other examples described here, but is predicted by King (1986) who suggests that fault bends are likely sites of fault nucleation.

Displacement variation along the fault on the right (Fig. 7) is more difficult to interpret, in part because neither tip point is identifiable, and in part because the displacement, although generally asymmetrical, is irregular. Certainly the fault is segmented, but whether the higher displacement minimum, for example, represents a barrier or link point is debatable. We believe that the extensive disharmonic, minor folding immediately below and above this minimum reflects the interference of tip zone folding as two minor faults approached each other.

The apparent absence of multiple nucleation points within the regional-scale thrusts is considered to be a reflection of the large displacements. In other words, if smaller faults did once exist and subsequently join, continued displacement on the new large fault would overwhelm any initial irregularities indicative of the original small faults. The jogs recognized in the displacement patterns of the Turner Valley and unnamed (Fig. 10) thrust may reflect such partly-masked irregularities. Alternatively, these internal irregularities may reflect lithological control of the displacement function.

Development of thrust ramps

In three of the four regional-scale thrusts examined, the nucleation point of the fault is seen to lie *above* the main décollement or the lower fault tip. These faults initiated within the footwall and propagated up toward the surface, and down to the lower flat. The displacement pattern along the Fire Trail Thrust (Fig. 8) is similar to the overall pattern along one of the microfaults in the deformed mylonite (Fig. 4) in that displacement is asymmetrical and skewed toward the higher tip. In

addition, the geometry of the Fire Trail Thrust mirrors that of the microfault in that both higher tips are oriented at a high angle to bedding and are associated with tip folds, and both faults flatten toward their respective lower sections. We interpret the displacement pattern along the Fire Trail Thrust to indicate an asymmetrical fault propagation about a nucleation point *above* the main décollement; the asymmetry of fault propagation is thought to reflect the anisotropy of fracture strength in the multilayered bedding.

Fold development as a function of displacement variation

As noted in the sample descriptions above, minor folding is associated with the faults. The most obvious folding is seen at the tip zones where it is assumed to be related to the relatively high displacement gradient. That is, in order to relieve the tip zone stresses that must accumulate at places of high displacement gradients the rocks deform over a volume around the tip. This phenomenon is well known both from structural geology (e.g. Williams & Chapman 1983) and seismology (e.g. King & Yielding 1984). The analysis presented here supports this model; in particular, the correspondence between displacement gradient and extent of tip zone folding is well seen along the Fire Trail Thrust (Fig. 8) and the microfaults within the mylonite (Fig. 4), where tip zone folding is well developed adjacent to high displacement gradients.

The relation between non-tip zone folds and the faults is less well understood. Two forms of folds may be distinguished: a fairly close to tight, overturned and split antiform–synform pair (e.g. along the left fault in the pop-up, Fig. 7; the 'Auburn' Thrust, Fig. 7; the Turner Valley Thrust, Fig. 9; and the unnamed thrust, Fig. 10), and a gentle, upright to steeply inclined flexure near the maximum displacement (e.g. both mylonite faults, Figs. 3 and 4; and in the hangingwall of the Fire Trail Thrust, Fig. 8, and footwall of the unnamed thrust, Fig. 10).

The origin of the close to tight fold type is unknown. It is possible that it represents a relatively old tip zone fold which has since been passed through by the fault and effectively stranded, or the fold may be the fundamental feature. That is, the fault may be a consequence of work hardening in the overturned limb of the fold leading to an increase in deviatoric stress, or may reflect a strain softened zone in which the strain rate is able to rapidly increase. Because of this uncertainty it may not be appropriate to label such features (as they often are) "fault-propagation folds" (term from Suppe 1985) but rather describe them geometrically or in non-genetic terms.

The nature of the gentle flexure may be recognized as a geometrical necessity related to the variable displacement function along the fault and the decrease in deformation in a direction perpendicular to the fault. A line drawing of the microfault within the mylonite shown in Fig. 4 (Fig. 5) emphasizes the position of this flexure adjacent to the maximum displacement and the absence of near-fault deformation between the flexure and the tip point. A similar flexure is noted in the footwall of the Wind River Thrust, Wyoming (through seismic reflection), at a depth thought to approximate the nucleation point (maximum displacement) (King & Brewer 1983). These authors make the analogy between this flexure and the clustered zone of aftershocks in the same relative position during the 1980 El Asnam earthquake, and attribute the formation of the flexure to the type of variable displacement function recorded during the El Asnam event. In addition, similar flexures have been observed adjacent to the maximum displacement along normal faults, and the origin is similarly ascribed to the variable displacement function (Barnett *et al.* 1987). It is worth emphasizing (as do Barnett *et al.* 1987) that this near-fault deformation is developed adjacent to planar faults (or planar segments) and does not necessarily reflect a non-planar fault geometry as is typically assumed during cross-section construction.

DISCUSSION AND IMPLICATIONS

Cross-section construction

The predominant displacement pattern obtained from our analyses of regional-scale thrusts is one of constant magnitude, or simple monotonic increase or decrease toward the surface tip. With the exception of well controlled cross-sections (e.g. Turner Valley Thrust, Fig. 10), the construction of these cross-sections must to a great extent reflect the bias in the mind of their author, or in the particular school of cross-section construction which he (or she) follows. The unknown displacement function along major faults may not be critical in problems where regional sedimentation patterns are of greatest interest. However, in situations where the detailed geometry of a thrust and associated fold (if any) is required, knowledge of the displacement function becomes critical. This begs the question, if the displacement function is unknown, what type of function is the most likely? If the reader believes (as we do) that geometrically self-similar structures are related by a causal process which is scale-invariant, then the evidence outlined in the preceding sections favours a displacement curve symmetrical about a maximum (nucleation point) above the main décollement where the geometry of the fault is planar (e.g. segments of the planar microfault within the mylonite, Fig. 3). This may also be the case for a symmetrical fault system such as a flat–ramp–flat. Displacement will be asymmetrical if the fault has an asymmetrical geometry, such as the flat–ramp form of the Fire Trail Thrust (Fig. 8) or the microfault within the mylonite (Fig. 4).

Thrust ramp development

The popular model for thrust ramp development has the thrust step off a basal décollement to cut up section and possibly flatten within a higher horizon. This

scenario tends to leave the footwall undeformed and inactive in the development of a thrust belt. The displacement analyses presented here suggest that thrusts initiate above a décollement and propagate both up and down. The mechanistic explanation was first proposed by Gretener (1972), and recently reiterated by Eisenstadt & DePaor (1987), who showed that a heterogeneously layered material will possess both a non-uniform strength profile, and variable permeability and porosity properties (and therefore fluid pressures) such that various horizons will be susceptible to fracture while others deform cohesively or not at all.

There are several other reasons, aside from the evidence described here, for preferring a scenario of thrust fault development whereby faults initiate above the basal décollement. If the depth of nucleation is controlled by the thermal structure and uniform layer rheologies, we might expect a constant depth of nucleation while the state of the system remains constant. In particular, if a fault tends to initiate at the level of the strength maximum (8–15 km), corresponding to the depth at which thermally induced deformation mechanisms begin to predominate over pressure-sensitive mechanisms, as suggested by King (1986), then propagation will occur both up and down. A modern (active) example of this was noted during the Corinth earthquake series of 1981 in which the aftershock distribution showed the fault to propagate both above and below the initiation depth (Vita-Finzi & King 1985). Also, the development and growth of kink bands and chevron folds (similar to faults in that both represent the sudden onset of instability) in deformation experiments in synthetic multilayers show similar multiple nucleation sites (and eventual coalescence) *within* the body of the material (e.g. Cobbold 1976).

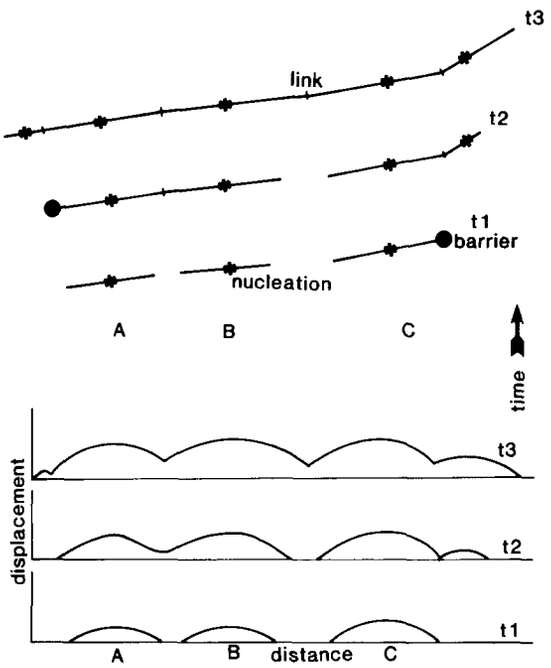

Fig. 11. Schematics of large thrust fault development. Three initially independent faults, A, B and C, have formed after $t1$ time, with the appropriate displacement functions shown in lower diagram. Note that C is (arbitrarily) slightly larger than A or B, suggesting that it formed prior to A and B or has propagated faster. A barrier exists (of unspecified character) at the right end of fault C. Further seismic slip occurs at $t2$ time, such that A and B link (notice the equal displacement magnitude for A and B faults). A new fault begins to the right of the barrier (with an appropriate smaller displacement function), and a new barrier exists at the left end of A. The process continues in like manner to time $t3$. This hypothetical example combines the processes of fault linkage, and propagation across barriers. Displacements are approximately self-similar in time.

Development of large thrust faults

The various displacement analyses presented here corroborate the hypothesis of thrust fault development through pervasive footwall deformation (assuming a foreland thrust migration model) and fault linkage (Gretener 1972), and that described by King & Yielding (1984) whereby thrusts propagate in segmented form, progressively overcoming barriers. Figure 11 describes a hypothetical scenario which involves the initiation and growth of three small faults. Each segment grows with time through the successive application of similar displacement functions, or characteristic earthquakes. Note that only the discontinuous displacement is shown in Fig. 11. The development of the fault system is shown to involve linkage of the initial segments, and impedance of growth by barriers. In detail, we find with King & Yielding (1984) that barriers are usually fault bends, but only in one example do we see evidence for nucleation at a fault bend. Fault bends are, with this exception, places of minimal displacement. It is apparent that, where displacements between minima and (or) tip points are of differing magnitudes, displacement analysis by itself is unable to distinguish between the continuously segmented faults (described by King & Yielding 1984), and independently segmented faults as described here. The distinction, however, between the processes of fault linkage, and propagation past barriers diminishes as the fault system matures, and as smaller faults coalesce.

The gradual accumulation of displacement (Fig. 11) gives rise to an apparently irregular pattern in which displacement minima and maxima are associated with points of linkage and nucleation, respectively. In this context we do not agree with Barnett *et al.* (1987) who claim that an irregular displacement function across a single fault is indicative of interpretative error or poor data (Barnett *et al.* 1987, p. 929). An alternative interpretation is that the single fault is a complex of previously shorter faults that have since linked.

CONCLUSIONS

Displacement variations along thrust faults of different sizes show a variety of patterns. Along real thrust faults (as opposed to those inferred or extrapolated to depth) displacements are irregular, with internal minima and maxima, indicating that large faults are segmented, and may develop through linkage of smaller faults, and (or) propagation across barriers (Fig. 11). Linkage

points or barriers are identified as fault bends. In addition, thrust faults usually nucleate and develop above the main décollement, and propagate both up toward the surface and down toward the flat, and do not step up from the basal décollement.

In the construction of cross-sections through folds and thrusts where the detailed geometry of the fault and (or) stratigraphy is poorly known, the displacement pattern most likely to give an accurate geometry is that which involved a symmetrical distribution about a maximum (nucleation). The asymmetry of the displacement function will reflect the asymmetry of the overall thrust fault, such that, for example, a flat–ramp geometry (e.g. Fire Trail Thrust, Fig. 8) will show a higher displacement–distance gradient toward the steeper tip.

Acknowledgements—We are grateful to our colleagues in the Department of Geology, University of Minnesota, Duluth, for helpful discussions and criticism. John Walsh and Juan Watterson provided particularly helpful reviews which considerably improved the manuscript. Thanks go to Paul Bodin who faultlessly introduced us to the 'characteristic earthquake', and also to an anonymous reviewer.

REFERENCES

Badgley, P. C. 1965. *Structural and Tectonic Principles*. Harper & Row, New York.

Barnett, J. A. M., Mortimer, J., Rippon, J. H., Walsh, J. J. & Watterson, J. 1987. Displacement geometry in the volume containing a single normal fault. *Bull. Am. Ass. Petrol. Geol.* **71**, 925–937.

Cobbold, P. R. 1976. Fold shapes as functions of progressive strain. *Phil. Trans. R. Soc. Lond.* **A283**, 129–138.

Dunlap, W. J. & Ellis, M. A. 1986. Fault nucleation and propagation: Evidence from thrust displacement analyses. *Geol. Soc. Am. Abs. w. Prog.* **18**, 590.

Eisenstadt, G. & DePaor, D. G. 1987. Alternative model of thrust-fault propagation. *Geology* **15**, 630-633.

Gallup, W. B. 1951. Geology of the Turner Valley oil and gas field, Alberta, Canada. *Bull. Am. Ass. Petrol. Geol.* **35**, 797–821.

Gordy, P. L. & Ferry, F. R. 1975. Geological cross-sections and composite seismic sections through the Foothills. In: *Structural Geology of the Foothills Between Savanna Creek and Panther River, S.W. Alberta, Canada* (edited by Evers, H. J. & Thorpe, J. E.). Canadian Society of Petroleum Geologists–Canadian Society of Exploration Geophysics, Calgary.

Gretener, P. E. 1972. Thoughts on overthrust faulting in a layered sequence. *Bull. Can. Petrol. Geol.* **20**, 583–607.

King, G. C. P. 1986. Speculations on the geometry of the initiation and termination processes of earthquake rupture and its relation to morphology and geological structure. *Pure Appl. Geophys.* **124**, 567–585.

King, G. C. P. & Brewer, J. 1983. Fault related folding near the Wind River thrust, Wyoming, *Nature* **306**, 147–150.

King, G. & Yielding, G. 1984. The evolution of a thrust fault system: processes of rupture initiation, propagation and termination in the 1980 El Asnam (Algeria) earthquake. *Geophys. J. R. astr. Soc.* **77**, 915–933.

Mudge, M. R. 1972. Structural geology of the Sun River canyon and adjacent areas, northwestern Montana. *Geol. Survey Prof. Paper* **663-B**, 52.

Muraoka, H. & Kamata, H. 1983. Displacement distribution along minor fault traces. *J. Struct. Geol.* **5**, 483–495.

Price, R. A. & Fermor, P. R. 1982. Structure section of the Cordilleran foreland thrust and fold belt, west of Calgary, Alberta. *Geological Survey of Canada*, Open File 882.

Royse, F. J., Warner, M. J. & Reese, D. C. 1975. Thrust belt structural geometry and related stratigraphic problems, Wyoming–Idaho–northern Utah: Rocky Mtn. Assoc. Geol., Symposium on deep drilling frontiers in the central Rocky mountains, 41–54.

Schwartz, D. P., Coppersmith, K. J., Swan III, F. H., Somerville, P. & Savage, W. U. 1981. Characteristic earthquakes on intraplate normal faults (abstract). *Earthquake Notes* **52**, 71.

Suppe, J. 1985. *Principles of Structural Geology*. Prentice-Hall, Englewood Cliffs, U.S.A.

Vita-Finzi, C. & King, G. C. P. 1985. The seismicity, geomorphology, and structural evolution of the Corinth area of Greece. *Phil. Trans. R. Soc. Lond.* **A314**, 379–407.

Watterson, J. 1986. Fault dimensions, displacements and growth. *Pure Appl. Geophys.* **124**, 365–373.

Williams, G. & Chapman, T. 1983. Strains developed in the hanging-walls of thrusts due to their slip/proportion rate: a dislocation model. *J. Struct. Geol.* **5**, 563–571.